Eur. Phys. J. D **38**, 277–283 (2006)
DOI: 10.1140/epjd/e2006-00058-6

THE EUROPEAN PHYSICAL JOURNAL D

# Alternate technique for simultaneous measurement of photoionization cross-section of isotopes by TOF mass spectrometer

M. Saleem, N. Amin, S. Hussain, M. Rafiq, S. Mahmood, and M.A. Baig[a]

Atomic and Molecular Physics Laboratory, Department of Physics, Quaid-i-Azam University, Islamabad, Pakistan

Received 21 October 2005 / Received in final form 30 November 2005
Published online 21 March 2006 – 

**Abstract.** New measurements of photoionization cross-sections of the lithium isotopes are reported employing a Time of Flight (TOF) mass spectrometer in conjunction with an atomic beam apparatus. Using a two-step selective photoionization and saturation technique, we have simultaneously measured the photoionization cross-section of the $2p$ excited state of both the isotopes $Li^6$ and $Li^7$ as $15 \pm 2.5$ Mb and $18 \pm 2.5$ Mb where as the corresponding number densities have been determined as $N_0 \approx 5.3 \times 10^{10}$ atoms/cm$^3$ and $N_0 \approx 6.2 \times 10^{11}$ atoms/cm$^3$ respectively.

**PACS.** 32.80.-t Photon interactions with atoms – 32.80.Cy Atomic scattering, cross-sections, and form factors; Compton scattering – 32.80.Dz Autoionization

## 1 Introduction

Lithium possesses two isotopes, $Li^6$ (7.5%) and $Li^7$ (92.5%). The $Li^6$ is the most important isotope because of its use to bread tritium, which reacts with deuterium to produce energy in the fusion reactors. Similarly $Li^7$ enriched over 99.9% is used for PH control in the PWR type fission reactors. For high isotopic purity, laser based methods for the isotope separations are very attractive. Bernhardt et al. [1,2] successfully separated the isotopes of barium by laser deflection method. Shimazu et al. [3] suggested the feasibility of separating lithium isotopes by two step photoionization. Karlov et al. [4,5] applied two step selective photoionization technique for the isotope separation of Nd, Sm, Eu, Gd, Dy, Er, Li and U, etc. Yamashita et al. [6] registered a patent for the isotope separation of lithium using two step photoionization technique. Arisawa et al. [7,8] used the same technique for the lithium isotope separation and obtained highly enriched $Li^6$ by tuning a laser to the $^2P_{1/2}$ state of $Li^6$. Mariella [9] registered a patent for the isotope separation of lithium using solar radiations to ionize the excited isotopes. Arisawa et al. [10] also proposed the lithium isotope separation by laser enhanced chemical reaction. Balz et al. [11] separated the lithium isotopes by double resonance enhanced multiphoton ionization of $Li_2$. Maruyama et al. [12] separated the titanium isotopes using two step photoionization method. Olivares et al. [13,14] applied the two step photoionization technique for lithium isotope separation and resolved the doublets of $Li^6(^2P_{1/2}, {}^2P_{3/2})$ and $Li^7(^2P_{1/2}, {}^2P_{3/2})$. All the methods described above require a very narrow bandwidth exciter dye laser. However, a Time of Flight (TOF) mass spectrometer in conjunction with an atomic beam system offers the possibility of isotope separation even if they have not been selectively excited. The enrichment of any selective isotope can be quantified if the photoionization cross-section of the energy level that is being used for the selective excitation is known exactly.

The experimental method of the photoionization cross-section measurement based on the observation of saturation in ion yields as a function of intensity of the ionizing radiation was first proposed by Ambartzumian et al. [15]. They measured the photoionization cross-section for the 6 $^2P_{3/2}$ and 6 $^2P_{1/2}$ states of Rb atoms. Later on, this method was improved and used with success by Heinzmann et al. [16] and Nygaard et al. [17] to measure the photoionization of 6 $^2P_{3/2}$ and 6 $^2P_{1/2}$ states of cesium. Bradley et al. [18] employed same technique and measured the cross-section of the autoionization resonance of Mg $3s3p(^1P^o_1) \rightarrow 3p^2(^1S_0)$. Subsequently, Burkhardt et al. [19] determined the magnitude of the phoionization cross-section and the atomic density for the resonance levels of sodium, barium and potassium by utilizing the saturation technique. They used one laser to excite the atoms to the resonance level and a second laser for a complete ionization of the excited atoms. Mende et al. [20] further improved the theoretical part by taking the Gaussian distribution function for determining the photon flux and measured the photoionization cross-section of Sr $(5s5p)^1P_1$ state. Lithium being an important element has been studied extensively for the

[a] e-mail: baig@qau.edu.pk

measurement of the photoionization cross-section of the $2p$ resonant level, by theoretical groups [21–25] as well as experimental [7,26–28]. Moskvin [21] calculated theoretically the photoionization cross-section of lithium atom by quantum defect theory as 15.7 Mb and Ya'akobi [22] calculated employing the same theory as 16.7 Mb at threshold ionization energy. Using the self consistent field approximation Gezalov and Ivanova [23] calculated the photoionization cross-section of the $2p$ level as 15.0 Mb for the same threshold ionization energy. Aymar et al. [24] calculated the photoionization cross-section for $s$, $p$ and $d$ Rydberg states of lithium, sodium and potassium using parametric central potential in the framework of single electron non-relativistic model. They calculated the value of the cross-section for lithium at $2p$ as 15.2 Mb at threshold ionizing energy. Lahiri and Manson [25] using the central-potential model calculated the cross-section of lithium atom for $s$ and $p$ states. They quoted the value at $2p$ as 14 Mb at energy 0.009 Ry above the ionization potential.

The first experimental value for the photoionization cross-section of lithium atom at $2p$ was reported by Rothe [26] as $19.7 \pm 3$ Mb at the threshold wavelength 350 nm using radiative electron-ion recombination of the emission spectrum of lithium plasma into the $2p^2P_{1/2,3/2}$ states. Karlov et al. [27] quoted this value as $10 \pm 3$ Mb at 337.1 nm using saturation technique, which is slightly less than that quoted by Lahiri and Manson [25]. Arisawa et al. [7] separated the isotopes of lithium and measured the cross-section of photoionization of $Li^6$ as (5–30) Mb by saturating the $2p\ ^2P_{1/2}$ excited state using the ionizing laser at 266 nm. Lahiri and Manson [25] using the central-potential model calculated the cross-section of lithium atom for $s$ and $p$ states. They quoted the value at $2p$ as 14 Mb at energy 0.009 Ry above the ionization potential, which is slightly higher than that quoted by Karlov et al. [27] at 337.1 nm ionizing laser. Magneto-optical traps are used for cooling and trapping the atoms and Wippel et al. [28] used this apparatus for the measurement of the photoionization cross-section of the first excited states of sodium atom and isotopes of lithium separately. Using saturation technique, they measured the photoionization cross-section of lithium isotopes at $2p$ as 6(– 5, + 20) Mb for $Li^6$ and $18.3 \pm 2.8$ Mb for $Li^7$ at 335.8 nm.

The present paper describes the isotope separation of lithium, calibration of a TOF detector for measuring the relative abundance of isotopes, dependence of the intensity of the photoion spectrum of lithium isotopes on the energy density of the ionizer that yield the corresponding photoionization cross-section of $Li^6$ and $Li^7$. The extracted values are in good agreement to that reported by Wippel et al. [28] using MOT technique.

## 2 Laser excitation scheme

An energy level diagram for the two-step resonance ionization of lithium isotopes illustrating red and UV radiation [13] is shown in Figure 1. Both isotopes of lithium have doublets and fine structures caused by the non-zero nuclear spin ($I = 1$ for $Li^6$ and $I = 3/2$ for $Li^7$), the separation between the $^2P_{3/2}$ state of $Li^6$ and the $^2P_{1/2}$ state of $Li^7$ is only 0.001 nm which is much smaller than the isotope shift, 0.015 nm. Therefore, a narrow line width laser and a well-collimated atomic beam are required to selectively excite the lithium isotopes from the ground state ($^2S_{1/2}$) to each of the doublet $^2P_{1/2}$ or $^2P_{3/2}$ components. The line width of our exciter laser is 0.00899 nm (0.2 $cm^{-1}$) that should excite the isotopes separately. However, we observed excitation of both the isotopes from the ground state by the exciting laser at 670.8 nm, which may be attributed to the wings of laser pulse. The excited levels of both the isotopes are then ionized by a photon having wavelength shorter than 350.0 nm, and are separated on the time axis in the TOF mass spectrometer.

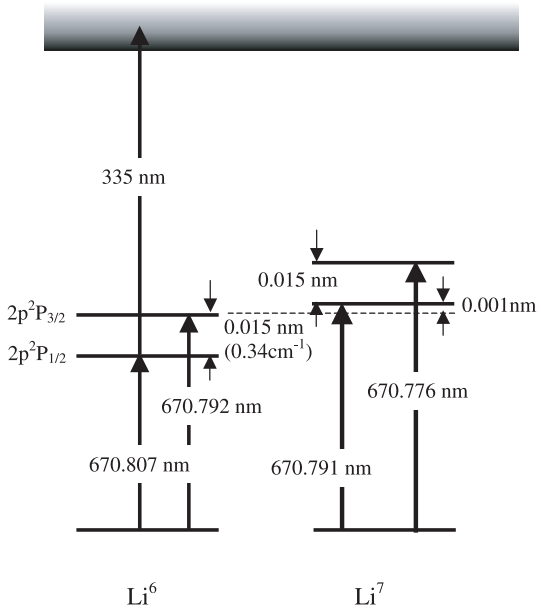


**Fig. 1.** Energy level diagram showing the two-step excitation and ionization paths for both the lithium isotopes.

## 3 Experimental details

The experimental apparatus contains a vacuum chamber, an exciter and ionizer dye laser (TDL 90, Quantel) and data recording system. The vacuum chamber consists of a lithium atomic beam apparatus and an in-house build TOF mass spectrometer, as shown in Figure 2a. The atomic beam apparatus consists of a stainless steel crucible of 9 mm inner diameter and depth of 75 mm, inserted in a stainless steal tube on which a thermo-coax wire (PHILIPS) is wrapped for resistively heating the sample. This assembly is again inserted in an alumina tube for electrical and resistive insulation. Atomic beam is emitted from a cap, 2 mm diameter hole and 0.5 mm wall thickness, fixed on the top of the crucible. An aperture of 2 mm diameter is installed above the exit hole of the crucible at a distance of 65 mm in order to get the collimated part of the atomic beam. The divergence of the atomic

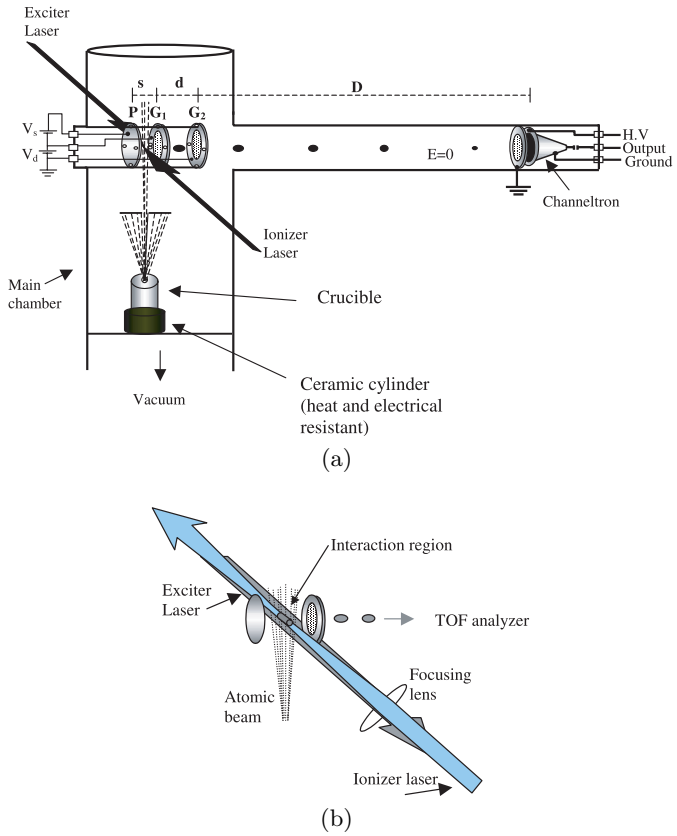


**Fig. 2.** (a) Atomic beam apparatus inside TOF mass spectrometer. TOF parameters: s = ionization/extraction region = 5 mm, d = acceleration region = 10 mm, D = field free drift length = 990 mm, P = accelerating grids, $G_1, G_2$ = accelerating grids, $E_s = V_s/s = 20$ V/mm, $E_d = V_d/d = 117.5$ V/mm. (b) Extended view of laser interaction with atomic beam.

beam was ≈61 mrad as measured from the spot of the lithium atomic beam on a glass strip fixed at ≈290 mm above the last aperture. At an operating temperature of 650 K for lithium, the mean free path $\lambda$ is ≈4 meter [29], which is much greater than the diameter of the exit orifice, ensures the flow of atoms through the exit hole in a transparent mode [30]. The number of lithium atoms effuse at this operating temperature from the exit hole is $\approx 6.2 \times 10^{14}$ atoms/s [29] and a constant number density of lithium atomic beam present in the interaction region after the collimation is $\approx 4.3 \times 10^{12}$ atoms/cm$^3$. The average velocity in the beam is found to be $1.4 \times 10^5$ cm/s [29] and the velocity component perpendicular to the atomic beam is $2.3 \times 10^3$ cm/s [2], that ensures a well-collimated atomic beam. This collimated beam coming from the downside passes through the ionization/extraction region of the TOF mass spectrometer, where it interacts with the exciter and ionizer lasers in orthogonal, as shown in Figure 2b. The TOF mass spectrometer with double field focusing [31] having one meter field free tube is build in-house (Fig. 2a). Interaction of the laser with the atomic beam via two-step ionization produces ions, which are resolved and measured in the TOF mass spectrometer.

The dye laser TDL-90 (Quantel) pumped by the second harmonic ($\lambda = 532$ nm) of the Nd:YAG laser (Brilliant) using the LDS698 dye dissolved in ethanol provided the resonance radiation ($\lambda = 670.8$ nm). The exciter laser radiation is frequency doubled ($\lambda = 335.4$ nm) from the same dye laser system in order to ionize the lithium atoms from the first excited state $2p\ ^2P_{1/2,\ 3/2}$. The line width of the exciter dye laser (≈0.2 cm$^{-1}$) is measured with an etalon having FSR 0.67 cm$^{-1}$. The exciter laser beam having a diameter of 4.5 mm filled the entire atomic beam diameter in the ionization/extraction region of the TOF mass spectrometer. The ionizer laser beam is focused at the center of the above mentioned region with a plano convex lens of 250 mm focal length to make the ionizing volume as nearly cylindrical as possible over the ion collection length (4.5 mm in our case, it is the calculated diameter of the atomic beam in the interaction region). Both the exciter and ionizer laser beams are combined at the center of the ionization/extraction region from opposite directions (Fig. 2b).

## 4 Results and discussions

The TOF distribution of lithium isotopes is recorded by the photoionization of the neutral lithium beam in two ways. First, the laser at 532 nm (32 mJ, 5 ns Pulse width) is focused on the lithium atomic beam that produces breakdown due to a high temperature achieved within a nanosecond of the laser pulse, as a result nearly 100% ionization is possible for all the species present in the focal volume [32]. It is therefore possible to generate the ions of lithium isotopes according to their natural abundance. These ions are then separated according to their mass to charge ratio in a TOF mass spectrometer, as shown in Figure 3. The detector voltage is optimized at 1300V for the linear mode operation. At this calibrated voltage, we observed the abundance of lithium isotopes in accordance to the literature cited values. Second, the photoions are produced by resonant two step (670.8 nm exciter + 335.4 nm ionizer), for the measurement of the photoionization cross-section of lithium isotopes. An expanded view of the well resolved isotopes is shown in Figure 3. A boxcar averaged two step photoionization signal of the lithium isotopes when the exciter laser is scanned from 668.8 nm to 672.8 nm is reproduced in Figure 4. The detector is operated in the linear mode in order to measure the data points for an accurate determination of the photoionization cross-section of lithium isotopes.

Figure 5 shows the dependence of the photoion current of $Li^6$ and Figure 6 of $Li^7$ on the ionizer laser energy density. These curves show that at low energy density of the ionizer laser, the dependence of the photoions current is linear and with an increase in the laser energy it deviates from the linearity and tends to saturate. Saturation is explained by the fact that at the high ionizing laser's energy, a total ionization of the excited atoms takes place and by increasing the laser energy further, the photoions current signal remains unaltered. The depletion rate by

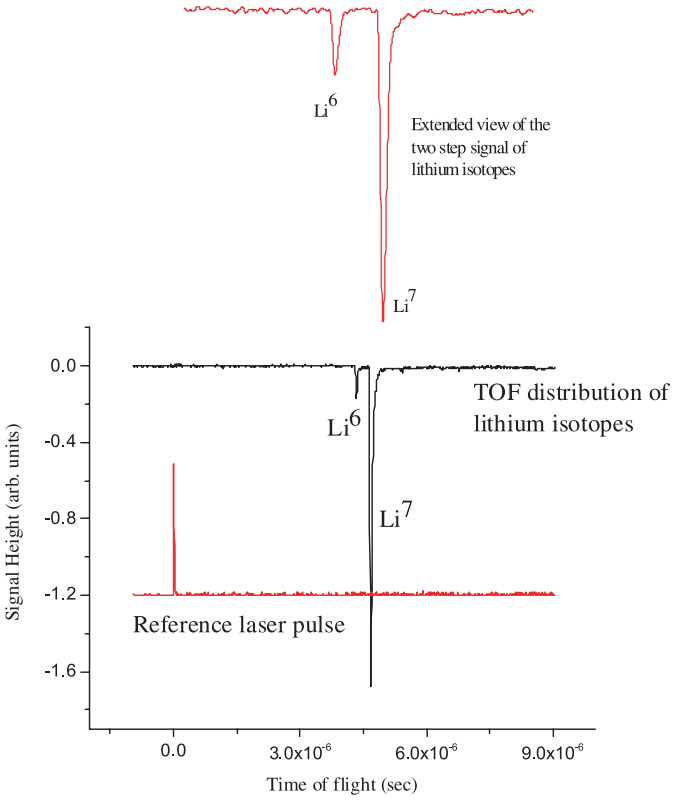


**Fig. 3.** Time of flight (TOF) distribution of lithium isotopes.

photoionization from a resonance quantum state $|\Psi_{excited}\rangle$ is represented as [19]:

$$\frac{dN_{excited}(t)}{dt} = -R_i N_{excited}(t) = -R_i \frac{N_{Total}(t)}{2}$$

where $R_i$ is the rate of photoionization, given by

$$R_i = \frac{I(t)\sigma}{\hbar\omega}$$

here $I(t)$ is the intensity of the ionizing laser pulse in (W/cm$^2$), $\sigma$ is the cross-section for photoionization of the resonance state $|\Psi_{excited}\rangle$ to all the accessible continuum states at this wavelength of the ionizing laser. The interaction of the ionizing laser with the lithium neutral atomic beam produces ions that are separated and detected in the TOF mass spectrometer. As a result the total ions produced per pulse are given as

$$\frac{Q}{e} = N_0 V \left[1 - \exp\left(-\frac{\sigma E}{2\hbar\omega A}\right)\right]. \qquad (1)$$

Here $Q$ is the total charge produced, $e$ is the electronic charge, $V$ is the laser-atomic beam interaction volume, as shown in Figure 2b, $A$ is the area of cross-section of the ionizing laser, $\hbar\omega$ is the energy of the ionizing photon, $E$ is the energy of the ionizing laser pulse and $N_0$ is the number density of ions in the ground state.

Equation (1) shows that the number of photoions gets saturated if the energy of the ionizing laser is infinite.

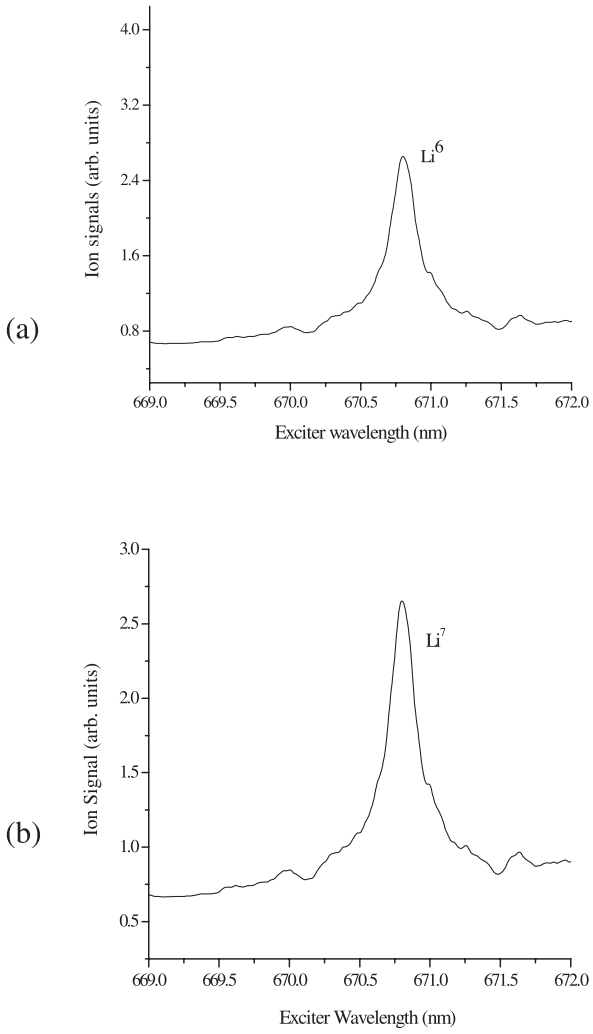


**Fig. 4.** Boxcar averaged signals of the lithium isotopes.

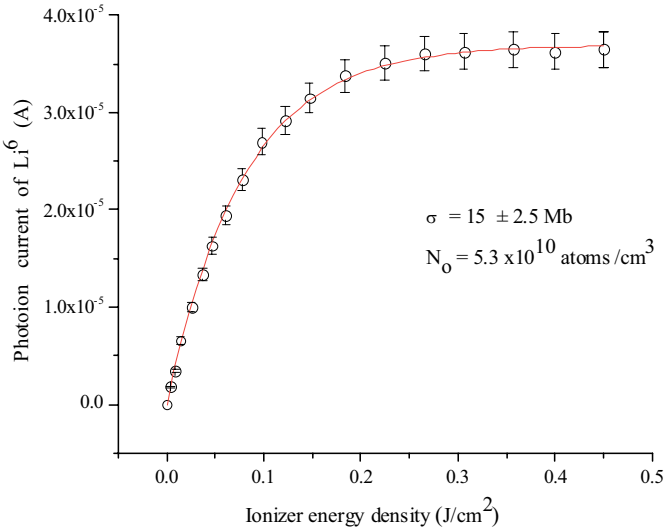


**Fig. 5.** The photoionization data for Li$^6$. The solid line is the least square fit of equation (1) to the observed data for extracting the values of the cross-section $\sigma$ (Mb) and number density (cm$^{-3}$) for $2p$ level of Li$^6$.

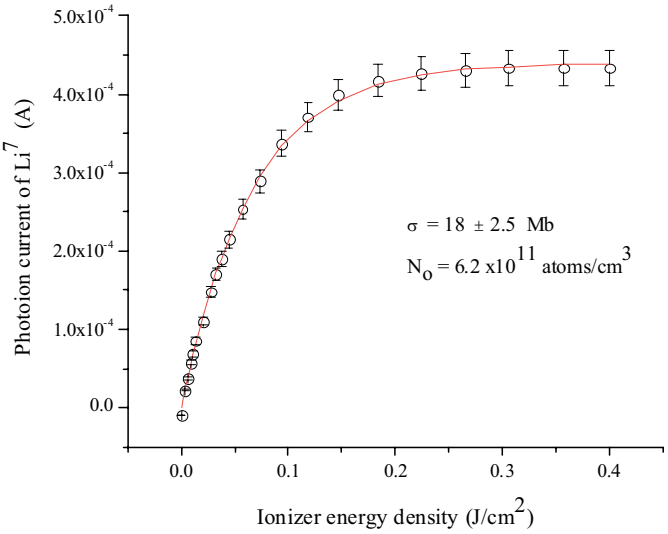


**Fig. 6.** The photoionization data for $Li^7$. The solid line is the least square fit of equation (1) to the observed data for extracting the values of the cross-section $\sigma$ (Mb) and number density ($cm^{-3}$) for $2p$ level of $Li^7$.

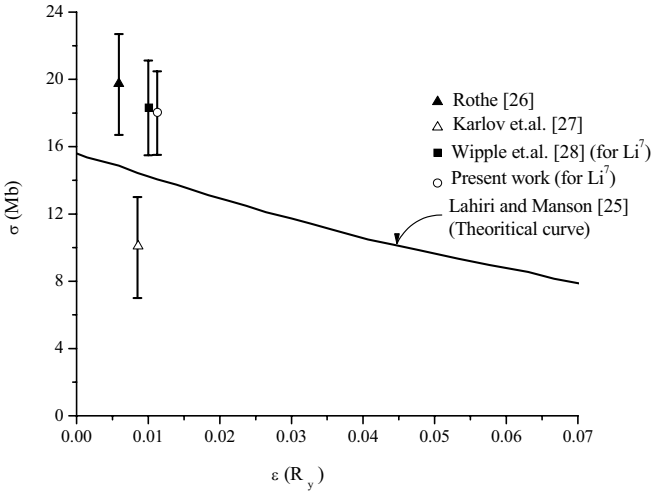


**Fig. 7.** Comparison of the experimental photoionization cross-section of lithium at $2p$ with the theoretical results.

However, every detection system has some limitations of sensing variations in the signal, that's why one may get saturated signal above a particular ionizing laser energy.

The correct value of the number density demands correct determination of the interaction volume defined by the overlap of the exciter and ionizer laser beams in the effective collection region along with the amplification of the detector, linearity of the detector including all electronics and the amplification of the detector. The interaction volume depends on the optical properties of the focusing lens and the geometry of the apparatus. The ionizing laser beam (335.4 nm) was focused to a diameter much smaller than that of the exciting laser beam by a long focal length lens chosen to make the ionizing volume as nearly cylindrical as possible over the ion collection length as defined by the lithium atomic beam diameter. By the combination of an iris aperture and focusing lens we managed to achieve nearly uniform laser beam intensity along the length of the interaction volume. This procedure also minimized the problems associated with the spatial overlap of the beams. Since both the laser beams originate from the same Nd:YAG laser, we nevertheless confirmed the temporal overlap with a photodiode. We have used a channeltron (4821G, Galileo) in the TOF mass spectrometer. The TOF detector produces voltage signals of lithium isotopes across a 50 Ω resistor, which can be converted to the number of ions produces accordingly

$$\frac{Q}{eV} = \frac{\left(\frac{Voltage\ signal}{R}\right)\Delta t}{eV}. \qquad (2)$$

Here $\Delta t$ is the pulse width of the ion signal in seconds. The lithium atoms are excited from their ground state $^2S_{1/2}$ to any of the doublet of $Li^6$ or $Li^7$ since the line width of our laser ($\approx$0.2 $cm^{-1}$) approaches the separation of $^2P_{3/2}$ of $Li^6$ and $^2P_{1/2}$ of $Li^7$. The laser prepared states of both lithium isotopes are then photoionized with the 335.4 nm ionizing laser. The signal heights of both the isotopes are recorded simultaneously by varying the intensity of the ionizing laser by inserting neutral density filters, keeping the intensity of the exciting laser fixed. The experimental data for the photoionization of the lithium isotopes $Li^6$ ($2p$) and $Li^7$ ($2p$) in Figures 5 and 6 are used to calculate the photoionization cross-section and number density by fitting these data in equation (1). For $Li^6$ ($2p$), it yields $\sigma = 15 \pm 2.5$ Mb and $N_0 = 5.3 \times 10^{10}$ atoms/$cm^3$ and for $Li^7$ ($2p$), the fitting procedure leads to $\sigma = 18 \pm 2.5$ Mb and $N_0 = 6.2 \times 10^{11}$ atoms/$cm^3$.

Our measured values of the photoionization cross-section of lithium isotopes are in good agreement with that reported in the literature. A comparison of the available experimental and theoretical data is presented in Figure 7. The continuous curve is taken from the theoretical work of Lahiri and Manson [25], which covers the energy from the first ionization threshold up to 0.3 Ry, whereas the experimental data points are confined to a small region above threshold. It is evident that the photoionization cross-section of $Li^7$ at $2p$ reported by Wippel et al. [28] is very close to the experimental value reported by Rothe [26] and the theoretical value reported by Lahiri and Manson [25]. Since $Li^7$ is around 92% of the isotopes of lithium, that is why the value reported by Wippel et al. [28] and by Rothe [26] are very close. The present measured value is also in good agreement to that reported by Wippel et al. [28] and Rothe [26]. All the available data on the photoionization cross-section of both the isotopes of lithium at $2p$ are tabulated in Table 1. The maximum overall uncertainty in the determination of the absolute cross-section is estimated 25%, which may be attributed to the experimental errors in the measurements of the laser energy and the cross-sectional area of the laser beam at the focusing volume. The values of the number density of both the isotopes $Li^6$ and $Li^7$ obtained by the curve fitting

**Table 1.** Quantitative comparison of photoionization cross-section data for lithium isotopes $Li^6$ and $Li^7$ at $2p$.

| Author | Method | $\sigma$(Mb) | |
|---|---|---|---|
| | | $Li^6$ | $Li^7$ |
| Arisawa et al. [7] | Saturation (atomic beam) | 5–30 ($\lambda = 266$ nm) | |
| Wippel et al. [28] | Saturation (MOT) | $15 \pm 15$ ($\lambda = 334.4$ nm)<br>$6(-5, +20)$ ($\lambda = 335.8$ nm) | $16 \pm 2.5$ ($\lambda = 334.4$ nm)<br>$18.3 \pm 2.8$ (at $\lambda = 335.8$ nm) |
| Present work | Saturation (TOF-Ms & atomic beam) | $15 \pm 2.5$ ($\lambda = 335.4$ nm) | $18 \pm 2.5$ ($\lambda = 335.4$ nm) |

are very close to their natural relative abundance. In order to obtain their actual number densities, we have divided the respective current signals with the detector gain. The total number density of both the isotopes in the interaction region is therefore $6.7 \times 10^{11}$ atoms/cm$^3$, which is not far from the calculated value $\approx 4.3 \times 10^{12}$ atoms/cm$^3$ [29]. This difference may be due to the uncertainty in the measurement of the signal heights, wastage of atoms due to scattering with the grids (having 90% optical transmission) and the collisions with other lithium atoms present in the atomic beam, as we have focused the ionizing laser at the center of the atomic beam. Some of the ions may be wasted due to the angles induced by the electrical lenses formed by the accelerating grids.

In conclusion, we have measured the photoionization cross-section of lithium isotopes at $2p$ using a TOF mass spectrometer because of its unmatched ion detection sensitivity [33] and the ability to resolve the isotopic masses. This instrument has the advantage over the atomic beam apparatus and thermionic diode detector that it made possible for simultaneous measurements of the spectroscopic properties of the constituent isotopes. This method can be used for all the elements provided the TOF mass spectrometer has sufficient resolving power. Sato et al. [34] investigated the single and double photoionization of Ca atoms using TOF mass spectrometer coupled with an atomic beam apparatus. Recently, it has been used for the measurement of single, double and triple photoionization cross-section of the ground state of lithium [35–38] using synchrotron radiations as the ionizing source. This method has also been used for the photo excitation studies of hollow lithium atoms [39,40]. Wehlitz et al. [41] used this instrument for the detection of single, double and triple isotopic ions of neon, lithium and beryllium produced by the synchrotron radiations. The same instrument has been used for the measurement of the photoionization cross-section of the excited states of nickel [42]. Gisselbrecht et al. [43] used it for the measurement of the absolute photoionization cross-section of the excited states of helium in the near threshold region. Samson et al. [44] employed this method for the measurement of the double photoionization cross-section of helium.

The present work was financially supported by the Higher Education Commission (HEC) and the Quaid-i-Azam University, Islamabad, Pakistan. M. Saleem, Nasir Amin, Shahid Hussain and M. Rafiq are particularly grateful to the HEC for the grant of Ph.D. scholarship under the Merit scholarship scheme 200, indigenous scheme 200 and indigenous scheme 5000 respectively.

## References

1. A.F. Bernhardt, D.E. Duerre, J.R. Simpson, L.L. Wood, Appl. Phys. Lett. **25**, 617 (1974)
2. A.F. Bernhardt, Appl. Phys. **9**, 19 (1976)
3. M. Shimazu, Y. Takubo, Y. Maeda, Jpn J. Appl. Phys. **16**, 1275 (1977)
4. N.V. Karlov, B.B. Krynetskii, V.A. Mishin, A.M. Prokhorov, Appl. Opt. **17**, 856 (1978)
5. N.V. Karlov, B.B. Krynetskii, V.A. Mishin, A.M. Prokhorov, Sov. Phys. Usp. **22**, 220 (1979)
6. M. Yamashita, H. Kashiwagi, U.S. patent 4,149,077 (10 April 1979)
7. T. Arisawa, Y. Maruyama, Y. Suzuki, K. Shiba, Appl. Phys. B **28**, 73 (1982)
8. T. Arisawa, Y. Suzuki, Y. Maruyama, K. Shiba, J. Phys. D: Appl. Phys. **15**, 1955 (1982)
9. R.P. Mariella, U.S. patent 4,320,300 (16 March 1982)
10. T. Arisawa, Y. Suzuki, Y. Maruyama, K. Shiba, Chem. Phys. **81**, 473 (1983)
11. J.G. Balz, R.A. Bernheim, L.P. Gold, J. Chem. Phys. **86**, 6 (1987)
12. Y. Maruyama, Y. Suzuki, T. Arisawa, K. Shiba, Appl. Phys. B **44**, 163 (1987)
13. I.E. Olivares, A.E. Duarte, Appl. Opt. **38**, 7481 (1999)
14. I.E. Olivares, A.E. Duarte, E.A. Saravia, F.J. Duarte, Appl. Opt. **41**, 2973 (2002)
15. R.V. Ambartzumian, N.P. Furzikov, V.S. Letokhov, A.A. Puretsky, Appl. Phys. **9**, 335 (1976)
16. U. Heinzmann, D. Schinkowski, H.D. Zeman, Appl. Phys. **12**, 113 (1977)
17. K.J. Nygaard, R.E. Hebner, J.D. Jones, R.J. Corbin, Phys. Rev. A **12**, 1440 (1975)
18. D.J. Bradley, C.H. Dudan, P. Ewart, A.F. Purdie, Phys. Rev. A **13**, 1416 (1976)
19. C.E. Burkhardt, J.L. Libbert, Jian Xu, J.J. Leventhal, Phys. Rev. A **38**, 5949 (1988)
20. W. Mende, K. Bartschat, M. Kock, J. Phys. B: At. Mol. Opt. Phys. **28**, 2385 (1995)
21. Yu. V. Moskvin, Opt. Spectrosc. **15**, 316 (1963)
22. B. Ya'akobi, Pro. Phys. Sov. **92**, 100 (1967)
23. Kh. B. Gezalov, A.V. Ivanova, High Temp. **6**, 400 (1968)
24. M. Aymar, E. Luc-Koenig, F. Combet Farnoux, J. Phys. B: At. Mol. Phys. **9**, 1279 (1976)
25. J. Lahiri, S.T. Manson, Phys. Rev. A **48**, 3674 (1993)

26. D.E. Rothe, J. Quant. Spectrosc. Radiat. Transfer **11**, 355 (1971)
27. N.V. Karlov, B.B. Krynetskii, O.M. Stel'makh, Sov. J. Quant. Electron. **7**, 1305 (1977)
28. V. Wippel, C. Binder, W. Huber, L. Windholz, M. Allegrini, F. Fuso, E. Arimondo, Eur. Phys. J. D **17**, 285 (2001)
29. N.F. Ramsey, *Molecular Beams* (Oxford Press, 1956)
30. K.J. Ross, B. Sonntag, Rev. Sci. Instrum. **66**, 4409 (1995)
31. W.C. Wiley, I.H. McLaren, Rev. Sci. Instrum. **26**, 1150 (1955)
32. J.F. Ready, J. Appl. Phys. **36**, 462 (1965)
33. M.J. Castaldi, S.M. Senkan, J. Air Waste Manag. Assoc. **48**, 77 (1998)
34. Y. Sato, T. Hayaishi, Y. Itikawa, Y. Itoh, J. Murakami, T. Nagata, T. Sasaki, B. Sonntag, A. Yagishita, M. Yoshino, J. Phys. B: At. Mol. Phys. **18**, 225 (1985)
35. M.-T. Huang, R. Wehlitz, Y. Azuma, L. Pibida, I.A. Sellin, J.W. Cooper, M. Koide, H. Ishijima, T. Nagata, Phy. Rev. A **59**, 3397 (1999)
36. R. Wehlitz, J.B. Bluett, S.B. Whitfield, Phys. Rev. A **66**, 012701
37. H.W. van der Hart, C.H. Greene, Phys. Rev. Lett. **81**, 4333 (1998)
38. R. Wehlitz, M.-T. Huang, B.D. Depaola, J.C. Levin, I.A. Sellin, T. Nagata, J.W. Cooper, Y. Azuma, Phys. Rev. Lett. **81**, 1813 (1998)
39. Y. Azuma, S. Hasegawa, F. Koike, G. Kutluk, T. Nagata, E. Shigemasa, A. Yagishita, I.A. Sellin, Phys. Rev. Lett. **74**, 3768 (1995)
40. Y. Azuma, F. Koike, J.W. Cooper, T. Nagata, G. Kutluk, E. Shigemasa, R. Wehlitz, I.A. Sellin, Phys. Rev. Lett. **79**, 2419 (1997)
41. R Wehlitz, D. Luckić, C. Koncz, I.A. Sellin, Rev. Sci. Instrum. **73**, 1671 (2002)
42. P. Lievens, E. Vandeweert, P. Thoen, R.E. Silverans, Phys. Rev. A **54**, 2253 (1996)
43. M. Gisselbrecht, D. Descamps, C. Lynga, A. L'Huillier, C.-G. Wahlstrøm, M. Meyer, Phys. Rev. Lett. **82**, 4607 (1999)
44. J.A.R. Samson, W.C. Stolte, Z.–X. He, J.N. Cutler, Y. Lu, Phys. Rev. A **57**, 1906 (1998)